American Mineralogist, Volume 77, pages 336–344, 1992

Transmission electron microscopic investigation of fission tracks in fluorapatite

Tracy A. Paul, Paul G. Fitzgerald
Department of Geology, Arizona State University, Tempe, Arizona 85287, U.S.A.

Abstract

Induced fission tracks have been imaged in fluorapatite with a JEOL JEM-2000FX analytical transmission electron microscope that is equipped with a cold stage and anti-contamination device. Near the atomic level, fission tracks are not perfectly linear, continuous features but are composed of segments of extended damage that are separated by gaps of undamaged microstructure. From dark-field TEM images, it appears that the damage around tracks is not extensive. Track width is crystallographically controlled. Parallel to the c axis, tracks display widths of 5–13 nm and hexagonal faceting parallel to [0001]. Tracks perpendicular to the c axis display widths of 3–9 nm. Track annealing can be observed in situ by adjusting the heating current to the cold stage. The annealing of induced fission tracks in fluorapatite in the microscope is dependent on the current density of the specimen (i.e., radiolytic annealing) and the temperature of the specimen (i.e., thermal annealing). Track annealing is characterized by initial shortening from the track ends, followed by the development of gaps 4–100 nm wide along the track length that appear to represent restored microstructure. The rate at which individual tracks anneal is variable and may reflect differences in track orientation, grain composition, and degree of initial partial annealing.

Introduction

Fission tracks are microscopic defects that occur in insulating solids and represent radiation damage caused primarily by the fission of ^{238}U impurities (Fleischer et al., 1975). Fission-track analysis is a widely used method for dating a variety of minerals and glasses (e.g., Fleischer et al., 1975; Hepburn and Windle, 1980). Whereas apatite, zircon, and sphene are routinely examined for fission-track analyses, apatite $Ca_5(PO_4)_3(OH,F,Cl)$ is the most useful mineral to analyze because the temperature range over which fission tracks are retained in apatite (~110–150 °C for cooling rates of 0.1 to 10 °C/m.y.) can be applied to the resolution of a number of upper crustal geologic problems. In addition, the measurement of confined track length distributions in apatite (Gleadow et al., 1986a, 1986b), plus a wealth of annealing data and kinetic models for fission tracks in apatite (e.g., Green et al., 1989; Carlson, 1990), allows constraints to be placed on the thermal history of samples containing apatite. Common applications of apatite fission-track analysis include hydrocarbon exploration (e.g., Naeser, 1979; Gleadow et al., 1983) and tectonic uplift and thermal histories (e.g., Fitzgerald and Gleadow, 1990).

Using transmission electron microscopy (TEM) to examine mica, Silk and Barnes (1959) showed that heavy-charged particles passing through insulating solids created tracks of radiation damage. TEM observation of particle tracks was difficult because images of the tracks quickly faded while being observed under the electron beam. However, it was discovered that the latent tracks could be fixed and enlarged by chemical etching and hence could be observed with an optical microscope (Young, 1958; Price and Walker, 1962). It is this simple method of revealing radiation damage that made possible the development of fission-track analysis. However, by chemically removing the strained and reactive core of the track, evidence of the original registration process is lost. In addition, the core structure of unetched fission tracks may provide insight into the microstructural controls on track annealing processes. Whereas the importance of viewing fission tracks in their latent state has been recognized for 30 yr, atomic-scale characterization of the defect remains one of the least studied aspects of fission-track research. A recently developed experimental TEM technique can be used to observe unetched fission tracks in apatite (Paul, 1990; Paul and Fitzgerald, 1990).

This publication presents results of a TEM investigation into the atomic structure and annealing behavior of induced fission tracks in Durango apatite. Direct observation of latent fission tracks provides insight into the physical characteristics of tracks as well as information about track annealing mechanisms.

Experimental approach

Fluorapatite from Cerro De Mercado, Durango, Mexico, was chosen as the study material for the following reasons: (1) the geochemistry and geologic occurrence of the material is well known (Young et al., 1969), (2) the chemical composition of Durango apatite is representa-

0003–004X/92/0304–0336$02.00

tive of apatite derived from most igneous rocks (Seiber, 1986), (3) Durango apatite is used as an age-dating standard in fission-track laboratories throughout the world (Hurford, 1990), (4) the physical characteristics and annealing behavior of fission tracks in Durango apatite are well documented from optical microscope studies of chemically etched tracks (e.g., Green et al., 1986, 1989; Laslett et al., 1987; Duddy et al., 1988), and (5) large gem-quality single crystals of the material are readily available.

The number of naturally occurring fission tracks per unit area in Durango apatite ($\sim 10^5$ tracks/cm^2) is too small to make TEM observation feasible. Therefore, specimens were annealed at 450 °C for 5 h (Green et al., 1986) to remove totally preexisting tracks generated by the spontaneous fission of ^{238}U. A greater track density ($\sim 10^7$ tracks/cm^2) was then reintroduced into the crystal structure by irradiation in a nuclear reactor. Latent tracks in nature are produced by the spontaneous fission of ^{238}U, whereas the tracks studied in this investigation were produced by the thermal-neutron induced fission of ^{235}U. However, the similarity of the ^{235}U and the ^{238}U fission processes (Pappas et al., 1969; Draganic et al., 1989) suggests that fission tracks produced by the two nuclei are similar. Following irradiation, the sample was ground to a fine powder (average grain size = 10 μm^2), suspended in 95% acetone solution, and deposited on 3-mm diameter Cu TEM grids that had been coated with a holey carbon film.

TEM images of microstructural features were obtained through the interaction of high-energy (200 keV) electrons with the specimen. More than 10^6 electrons/nm^2 are typically required to obtain information on the identity and position of a single atom (Hobbs, 1987). Consequently, the beam current that is necessary to image atomic-scale defects, such as fission tracks, can cause significant sample degradation. At low operating voltages (less than 200 keV), degradation of apatite may be due to radiolytic decay. Above 400 keV, damage may be the result of a direct knock-on process. A JEOL JEM-2000FX analytical TEM with an optimal operating voltage of 200 keV was used in this study. Ion thinning, often necessary to prepare samples for TEM observation, can alter or destroy fission tracks (Fleischer et al., 1975) as well as severely damage the apatite structure. Therefore, samples are prepared as powdered grain mounts. Fortunately, an operating voltage of 200 keV allows observation of thick specimens, such as grains produced by the powdered grain mount technique. Consequently, the need to ion thin samples is eliminated, as sharp, bright images result even when viewing crystals greater than 200 nm in thickness. During their initial TEM investigation of fission tracks in natural mica, Price and Walker (1962) found that a cold stage was necessary if the tracks were to be observed over an extended period. The JEOL JEM-2000FX is equipped with a cold-stage specimen holder and an anticontamination device. These devices facilitate observation of long-term (1–300 min) in situ crystalline transformations (i.e., track annealing) and prevent contamination or mass loss in the specimen.

In addition to cooling the sample in order to prevent sample degradation, the electron beam current density impinging on the sample must be minimized. This requirement is accomplished through a combination of operating conditions: (1) the electron beam illumination is reduced with an aperture (~ 40 μm), (2) the grain image is formed from the Fourier transformation of only the direct beam, and (3) a holey carbon–coated Be grid is placed on top of the sample grid. The Be grid acts as a thermal and electron sink and therefore prevents sample charging and structural degradation during alignment of the electron beam as well as during high-resolution imaging.

Results and discussion

Fission-track characteristics

Following the approach described above, it is now possible routinely to observe unetched fission tracks in apatite at near atomic scale. Bright-field and dark-field TEM images illustrate the physical characteristics of fission tracks observed in this study.

The number of fission tracks per unit area induced in the sample material is calculated using the neutron dosimetry relation $n_f = {}^{235}N\phi\sigma(\mathrm{CR_U}/\mathrm{CR_U} - 1)t$, where n_f = number of induced fission events, ${}^{235}N$ = number of ^{235}U atoms, ϕ = neutron fluence, σ = probability cross section, $\mathrm{CR_U}$ = Cd ratio for U, and t = grain thickness (Green and Hurford, 1984). The Cd ratio for the V-43 position at the graphite reflector of the Georgia Institute of Technology nuclear reactor (Crowley, 1986) indicates that the contribution of epithermal neutron induced fission in ^{235}U is negligible. Therefore, use of the reduced track density equation is justified (for discussion of the approximation see Green and Hurford, 1984). The reduced track density equation is $n_f = {}^{235}N\phi\sigma t$ (Green and Hurford, 1984). For the apatite examined in this study, ${}^{235}N = 6.1 \times 10^{15}$ ^{235}U atoms/cm^3 (Young et al., 1969), $\phi = 1 \times 10^{17}$ neutrons/cm^2, $\sigma = 580.2 \times 10^{-24}$ cm^2 (Draganic et al., 1989), t = grain thickness (3×10^{-5} cm). Therefore, calculated $n_f = 1.1 \times 10^7$ track/cm^2. Induced fission-track volume densities observed in this TEM study are consistent with the calculated track volume density.

At the time of formation, fission tracks in apatite are approximately 22 μm in length (Donelick et al., 1990). Whole track lengths are, therefore, not encountered at TEM magnifications because the apatite grains observed in this study are less than 10 μm in the largest dimension. Observed track length segments are less than 5 μm. At magnifications less than 100 000×, fission tracks appear to be linear (Fig. 1A). However, at higher magnifications, the elastic-strain field around a track (Fig. 1B) displays a psuedosinusoidal geometry with a wavelength that approximates the track width. The irregular geometry of the track may be an important factor in annealing processes. As the psuedosinusoidal morphology develops from an

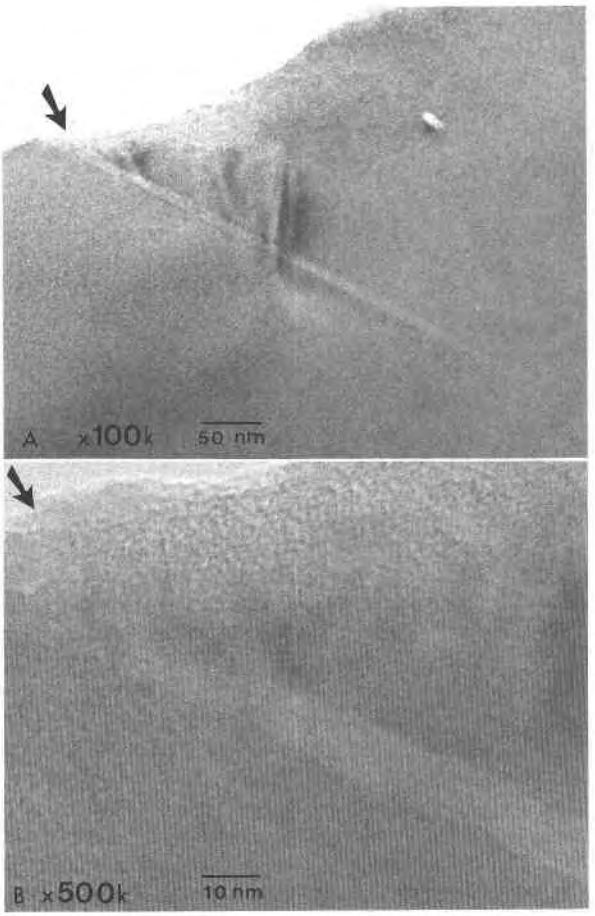

Fig. 1. (**A**) Confined fission tracks observed at magnifications less than 100 000× appear linear. (**B**) At greater magnifications (500 000×), the confined tracks display a psuedosinusoidal morphology. Lattice fringe images are approximately 45° to the track length and parallel to the **c** axis.

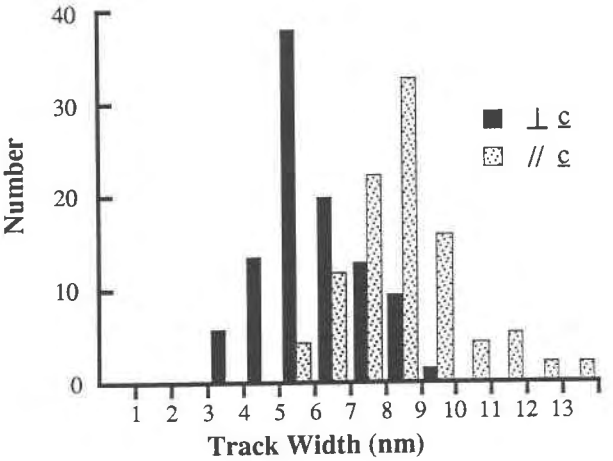

Fig. 2. Distribution of unetched confined fission-track width in fluorapatite, measured with respect to crystallographic direction. Normalized to 100. Total number of tracks measured is 293. Track width is crystallographically controlled, with tracks parallel to the **c** axis displaying larger widths than tracks perpendicular to the **c** axis.

initially linear track, the track volume decreases, the surface area and energy increases, and because activation energy is dependent on surface area size, it also increases. Hence, changes in track morphology, such as pinching of the track to create a psuedosinusoidal geometry or complete gaps (see the section on radiolytic annealing below), will effect the activation energies associated with annealing.

TEM images provide a two-dimensional view of a three-dimensional crystal structure. As a result, fission tracks confined within the crystal structure, as well as tracks that intersect or lie along the crystal surface, may be observed (see Gleadow et al., 1986b, for discussion of confined track characteristics). Using phase-contrast and bright-field TEM imaging conditions, tracks that are confined within "thin" grains appear brighter than tracks confined in "thick" grains. Fission tracks that are oriented at an angle to the grain surface in a wedge-shaped crystal become progressively brighter as the tracks approach the thinnest portions of the wedge. Therefore, the strain contrast around tracks that intersect or that are close to the grain surface is well defined, whereas the strain contrast around confined tracks appears more diffuse.

In order to eliminate the effect of surface intersection, track widths are only measured on confined tracks that are approximately parallel to the surface of the grain. Track widths imaged by this investigation range from 3 to 14 nm and average 5 and 9 nm perpendicular and parallel to the **c** axis, respectively (Fig. 2). This range is similar to those of the TEM observations of unetched particle tracks in mica (Silk and Barnes, 1959; Price and Walker, 1962) and in zircon (Bursill and Braunshausen, 1991). Induced fission tracks in apatite are revealed for optical analyses by chemically etching the apatite using 5N HNO_3 for 20 s. Under these etching conditions, the apparent track width increases 100–500 times, as etched fission tracks observed using a light microscope display widths on the order of 0.2–5.0 μm (200–5000 nm).

Transmission electron microscope observations can be used to evaluate the extent of radiation damage around a fission track in apatite. Dark-field images of fission tracks in apatite indicate that the intensity distribution of the elastic-strain field around the tracks is not extensive (Fig. 3). Bursill and Braunshausen (1991) found that heavy-ion irradiation (14 meV/u Pb ions) of zircon produced tracks whose elastic strain field diminished as a function of $\sim 1/r^2$. For reference, dislocation contrasts generally diminish at ranges of $1/r'$, where r' = the dislocation radius (Hull and Bacon, 1984). Although the extent of radial disruption of the crystal structure around a fission track is smaller than the disruption caused by a dislocation, the intensity of the disruption associated with fission tracks may be much greater. Whereas dislocations introduce an additional half plane of atoms into a crystalline

material and thereby distort the structure, fission fragments impart a large amount of kinetic energy to a crystal structure, leaving a trail of radiation damage that is hypothesized to consist of broken and rearranged bonds, Frankel defects, and antiphase domains (Fleischer et al., 1975). Lattice fringe images of confined fission tracks in apatite (30-nm grain thickness) are not distorted or offset (see Fig. 1), further suggesting that the damage zone around tracks, although intensive, is not extensive.

Induced fission tracks observed using TEM are not always continuous along their length. Individual tracks display variable degrees of continuity from essentially continuous to very discontinuous (Fig. 4). This phenomenon has also been reported for fission tracks in other solid-state detectors and may reflect changes in the fission-fragment energy (Hepburn and Windle, 1980; Dartyge et al., 1981). However, it should be noted that apparent discontinuity of track length can appear in TEM bright-field images as a consequence of irregular grain surfaces and variable grain thicknesses. Veritable discontinuity can be tested by tilting the sample in the transmission electron microscope. When tilted, apparent discontinuity is revealed as the full track length comes into contrast. Furthermore, in situ observation of annealing of tracks in apatite using TEM suggests that the extent of track length continuity can be influenced by partial annealing of the track. Fortunately, discontinuity caused by partial annealing has a unique appearance (see the section on radiolytic-thermal annealing below) that is easily discerned from discontinuity that is related to the initial formation of the track (see Fig. 4).

TEM observations suggest that fission-track width appears to be crystallographically controlled. Tracks parallel to the **c** axis display the largest average width, 9 nm, whereas tracks oriented with length perpendicular to the **c** axis display average widths of 5 nm (see Fig. 2). The observed width anisotropy may be a reflection of the anisotropic atomic structure of fluorapatite and may be a result of the structure's differential bond strengths. In the atomic structure of fluorapatite, five Ca atoms bond to each F atom forming a distorted trigonal bipyramid group. Ca atoms are shared by adjacent bipyramids and thereby link the groups into chains that are oriented parallel to the **c** axis. The electronegative behavior of F makes the chains strong. Perpendicular to the **c** axis, phosphate groups and Ca in sixfold coordination with O are bonded to one another and to the Ca-F groups by covalent sharing of O and to a lesser extent by long-range forces (McConnell, 1973; Zoltai and Stout, 1984; Hughes et al., 1990). As a result of the differential bond strength, defects that are introduced across the strong Ca-F chains (i.e., track length perpendicular to the **c** axis) must overcome a larger Peierl's force than defects that are introduced across the weaker intermolecular bonds (i.e., parallel to the **c** axis). Consequently, the largest track widths form in the direction in which it is easiest to disrupt the apatite structure ($\parallel$**c**) rather than in the direction in which a large amount of energy is required to overcome the bonding forces ($\perp$**c**). Observed track widths are also consistent with the elastic properties of Durango apatite (Yoon and Newnham, 1969). However, it should be noted that the elastic coefficients are valid only in regions of the crystal structure that are away from the track core. Parallel to the **c** axis and to the Ca-F chains, the elastic compliance of the crystal structure is small. As a result, after disruption by the fission fragment, the response of the crystal structure is large (i.e., involves the largest amount of rebound) and the retained track width is minimized. Con-

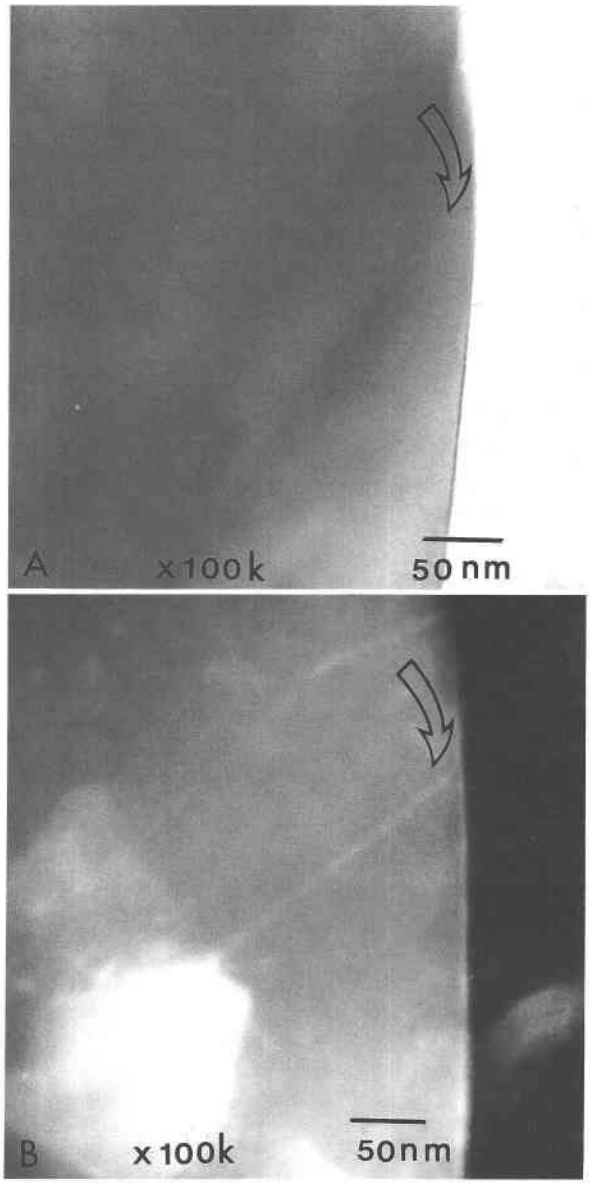

Fig. 3. (**A**) Using bright-field imaging conditions, the extent of elastic-strain contrast around a track in fluorapatite is small. Consequently, the track may not be completely visible. However, using dark-field imaging conditions (**B**), the track and associated strain may be better revealed.

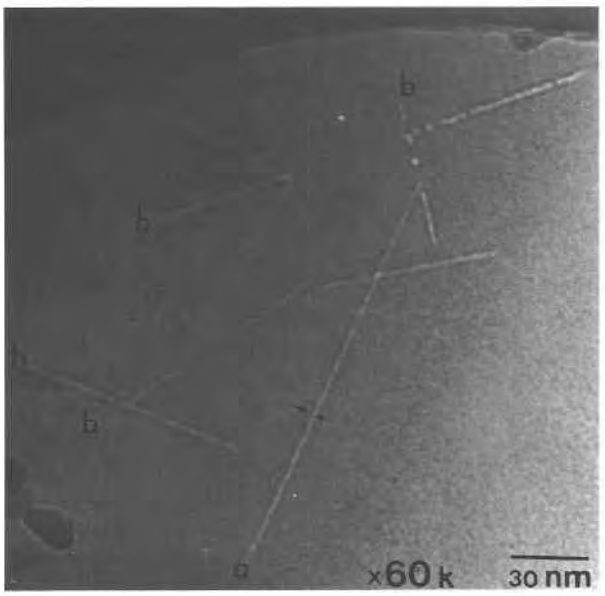

Fig. 4. Fission tracks in fluorapatite illustrating the variable degrees of continuity in fission-track length. Tracks labeled a are continuous, b are discontinuous. The elastic strain associated with a fission track is indicated by arrows.

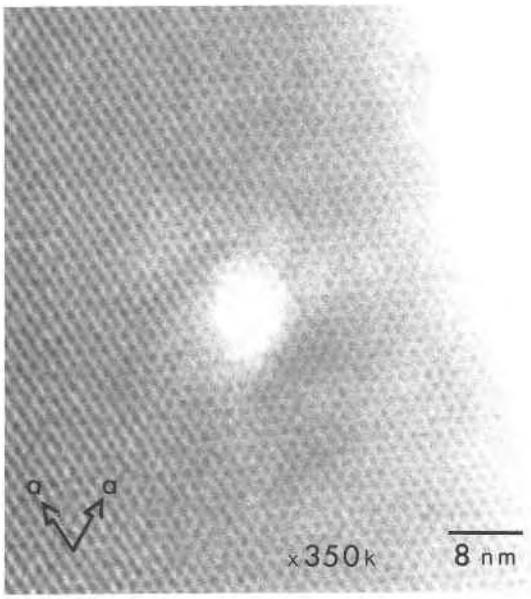

Fig. 5. Hexagonal faceting of a fission track cross section parallel to [0001] of fluorapatite.

versely, perpendicular to the **c** axis, compliance is large, the elastic response of the crystal structure near the track is small (i.e., little rebound), and the retained track width is large.

It is well known from studies of etched fission tracks in apatite that tracks parallel to the **c** axis anneal more slowly but etch faster than tracks perpendicular to the **c** axis (Green and Durrani, 1977; Green, 1981; Laslett et al., 1987; Donelick, 1991). Track annealing anisotropy may be controlled by track width anisotropy, with tracks parallel to the **c** axis requiring more time to anneal than tracks perpendicular to the **c** axis simply because they are physically wider. Observed etching rate anisotropy in apatite may also be a reflection of this observed difference in track width with crystallographic direction. Similarly, tracks parallel to the **c** axis display a larger etched width than tracks perpendicular to the **c** axis because they are physically wider prior to etching. Track width anisotropy may be better quantified and studied by using collimated fission tracks. Work on this subject is currently underway using a ^{252}Cf source.

Induced fission tracks in apatite have a variety of orientations and therefore display a variety of apparent cross-section geometries. Two observations suggest that unetched fission tracks are not cylindrical, as they are often idealized. First, the ranges in apparent width for both tracks parallel to the **c** axis and perpendicular to the **c** axis (see Fig. 2) suggest that track radius is not equal in all directions. Second, TEM images of tracks that are perpendicular to a crystal surface exhibit a cross-section geometry that reflects the symmetry of that crystal plane. Furthermore, the cross-sectional geometry of unetched tracks may be related to that of chemically etched tracks. For example, the cross section of tracks that are perpendicular to (0001) of fluorapatite exhibits hexagonal faceting (Fig. 5), while etched tracks at this orientation exhibit hexagonal etch pits. The cross-sectional geometry of both etched and unetched tracks reflects the lowest energy configuration for atoms in the intersecting plane.

The above discussion reflects a qualitative analysis of medium-resolution TEM observations of fission tracks in apatite. Additional high-resolution observations, following the work of Bursill and Braunshausen (1991) on zircon, should elucidate the nature of the defects in the fission-track core as well as the defect geometry and density.

In situ annealing experiments

The stability of induced fission tracks in Durango apatite in the transmission electron microscope is dependent on the current density of the specimen and the temperature of the specimen. We have classified the two effects as radiolytic and thermal annealing, respectively. Radiolytic annealing of fission tracks is induced by exposing the specimen to an electron beam. Thermal annealing can be induced by increasing the heating current to the cold stage. It should be noted that radiolytic annealing is not temperature independent nor is the temperature independent of the current density. Future in situ annealing experiments will address the interdependence of the two effects.

In order to control length and crystal direction biases, annealing experiments were conducted on apatite grains that display a minimum of five different track orientations and lengths. To ensure that significant partial annealing had not occurred prior to the experiment, the observed tracks were initially continuous in length when

viewed at a magnification of 100 000×. The film exposure time and image focus were fixed prior to the experiment in order to record changes in the elastic scattering of electrons. Apparent changes in track morphology caused by sample drift or tilt were excluded by recentering the SAED pattern prior to imaging. Both types of annealing, as well as their combined effects, were examined in this investigation as they may be suitable analogues for track annealing mechanism(s) observed in geologic environments.

Radiolytic annealing. The morphology of fission tracks changes when exposed to the electron beam. As beam exposure time increases, the continuity of the tracks along their length decreases. Gaps, 4–100 nm in length, develop along the track length and are indistinguishable from the apatite host, suggesting that they represent core regions of the fission track that have been restored to the original microstructure. Extended exposure to the electron beam does not completely anneal the tracks but instead degrades the apatite structure. Track morphology has been described as a continuous region of extended defects that are separated by gap zones of point defects (Dartyge et al., 1981). Studies of chemically etched tracks suggest that these gap zones anneal faster than the regions of extended defects (Dartyge et al., 1981; Green et al., 1986). TEM observations of radiolytic annealing of fission tracks in apatite confirm that gap zones exist (see Fig. 4) and that they are more susceptible to radiolytic annealing than other regions along the track. At present, it is unclear how the gaps observed using TEM are related to those described in etched track studies. Preservation of gaps in annealed and chemically etched tracks requires that the original gap be >1 μm in length (P. G. Green, personal communication, 1991). However, track segments observed using TEM are rarely longer than 1 μm.

Thermal annealing. It is well known from studies of etched fission tracks in apatite that track morphology changes in response to increasing temperature. Documentation and interpretation of in situ thermal annealing experiments using TEM are hindered by image-contrast effects that occur in response to sample heating (Hirsch et al., 1965). An increase in the heating current to the cold stage causes grains to drift and tilt. Initially, tracks appear to fade as a coherent feature. However, as the grain position and orientation change in response to the applied heating current, the image contrast varies and once-faded tracks are again visible. It is important to note that TEM observations of thermal annealing are difficult to compare with studies of chemically etched tracks in apatite. Experiments using etched tracks have determined that the rate of track annealing is dependent on time and temperature. Over geological time scales (i.e., tens of millions of years), the temperature at which fission tracks in fluorapatite are completely annealed is ~110 °C (Green et al., 1986). In laboratory furnace experiments of 1 h, fission tracks are completely annealed at 296 °C (Laslett et al., 1987). The maximum temperature at which annealing can be conducted in the ASU JEOL JEM-2000FX transmission electron microscope (~120 °C) requires unrealistically long experiment times in order to duplicate the extent of annealing that is produced in furnace experiments. Consequently, the comparison of annealing behavior observed using TEM with annealing studies employing etched tracks is tenuous. In fact, it is possible that thermal annealing as observed using TEM and as revealed by chemical etching of tracks are not correlated because healed gaps in a heavily annealed track may be blasted out by chemical etchant, giving an underestimate of the real amount of annealing that has occurred (Fig. 6).

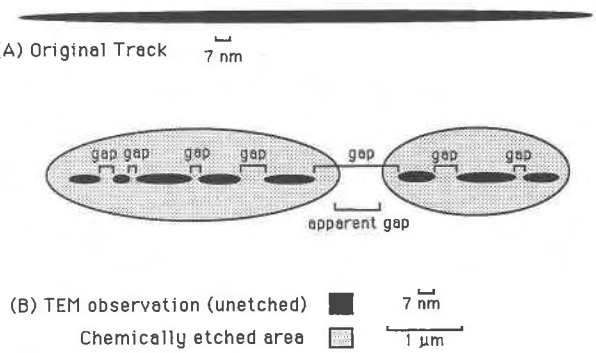

Fig. 6. (**A**) Schematic representation of initial fission-track morphology, observed using TEM. Scale approximate. (**B**) Schematic diagram of the morphology of partially annealed tracks observed after chemical etching superimposed with that of unetched partially annealed tracks observed using TEM. Note the appropriate scale bar associated with each method of observation. Numerous small gap zones along the track length are associated with partially annealed unetched tracks. However, these small gap zones are likely obliterated by chemical etching, and only large gap zones may be preserved. Consequently, the true extent of partial annealing may be underestimated in optical microscopy studies.

Radiolytic-thermal annealing. Radiolytic-thermal annealing is induced by setting the heating current to a constant value and allowing the sample temperature to increase while continuously exposing the sample to the electron beam. Figure 7 presents the results of a radiolytic-thermal annealing experiment. Under the imposed conditions, the observed annealing rate (percent decrease in track length/second) is not simply related to the heating rate (°C/second). The nonequivalence of the two rates reconfirms the susceptibility of fission tracks in apatite to radiolytic annealing.

Initially, the restoration of the microstructure in response to the combination of radiolytic and thermal annealing is fast. However, when the track length has been reduced by ~20% the rate of restoration slows. This change in rate is unqualified but may reflect a change in the dominant restoration mechanism. Radiolytic annealing of a track commences quickly but never results in the complete annealing of a track, regardless of the extent of electron beam exposure. In contrast, the changes associ-

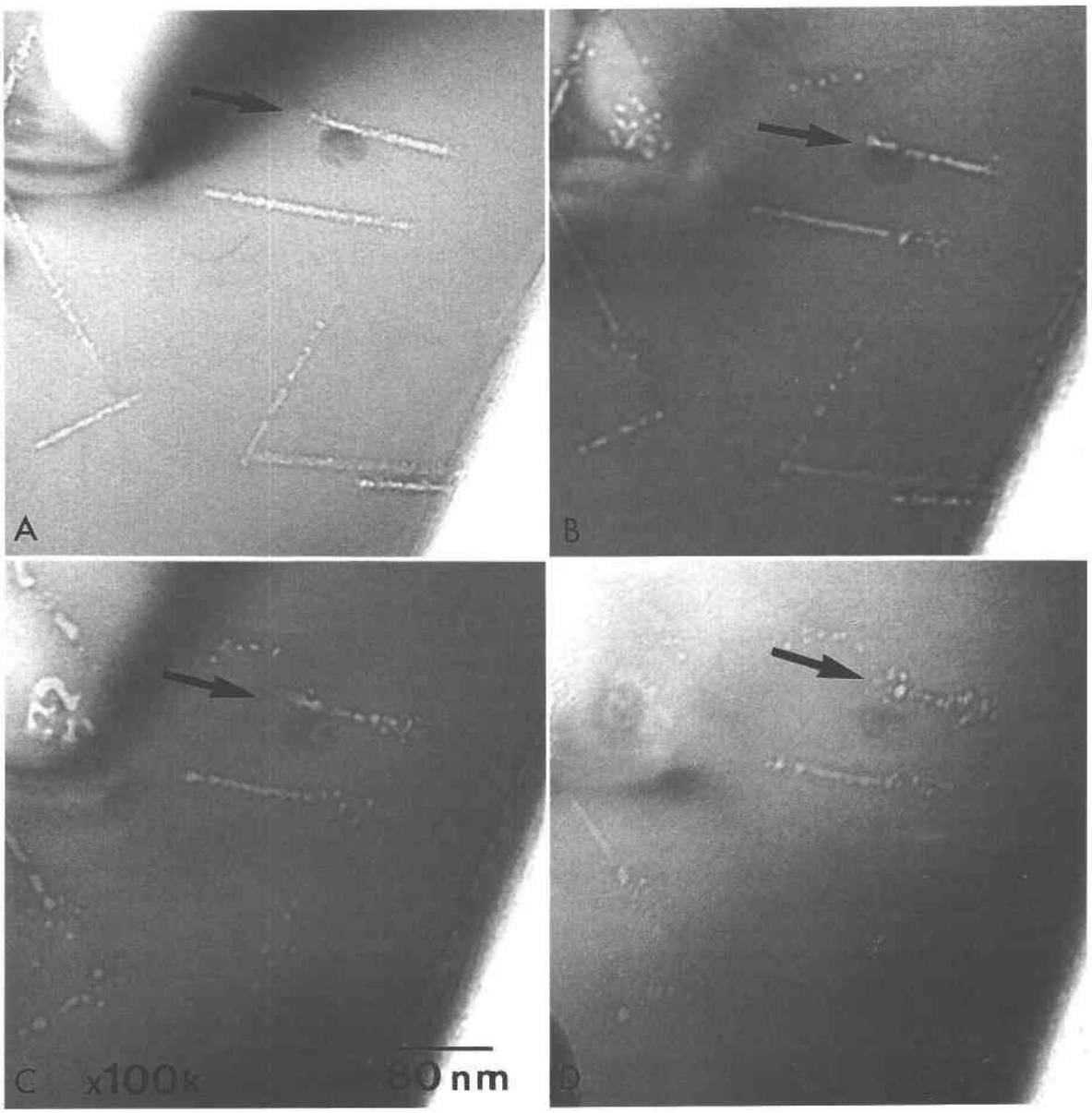

Fig. 7. Radiolytic-thermal annealing of induced fission tracks in fluorapatite. Beam current density ~0.35 A/cm². Constant heating current. (**A**) Initial sample temperature −175 °C. (**B**) After continuous electron-beam exposure and sample heating for 80 min (sample temperature −74 °C), the continuity of the reference track length decreases from the ends of the track (i.e., the intersections of the track with the surface of the grain). Track length is ~13% shorter. Small gaps (~3–10 nm) begin to develop along the track length. (**C**) After 140 min of electron-beam exposure and heating (sample temperature −26 °C), gaps are more distinctive (~4–15 nm) and length has now been reduced by ~19%. (**D**) After 180 min of electron-beam exposure and heating (sample temperature +75 °C), the reference track length is very discontinuous, the gap spacing is large (~9–25 nm), and the length has been reduced by ~38%. Additional heating makes track length so discontinuous that it is difficult to delineate or measure accurately.

ated with thermal annealing are not initially apparent and are visible only after the track has been heated for several hours. The existence of two annealing rates may reflect the change from initial dominance of a mechanism that is induced by the electron beam to that of a mechanism that is induced by an increase in temperature.

Conclusions

Insight into the physical characteristics of tracks, such as track morphology and continuity, width anisotropy, and radial damage, is possible from the TEM observation of fission tracks in apatite.

In situ annealing experiments using TEM indicate that fission-track stability is sensitive to both electron beam exposure and simple temperature increase. Annealing experiments conducted in the transmission electron microscope show that a change in annealing rate occurs with time. Whereas the difference in annealing rates associated with each process is reproducible, the annealing rates of individual tracks are variable and may reflect the influences reported in studies of chemically etched tracks, including track orientation, grain composition, and degree of prior partial annealing.

Whereas it is now possible to observe directly annealing of fission tracks in apatite, annealing remains a very complicated process to decipher (see Green et al., 1988). The interplay of thermal and radiolytic annealing mechanisms and the correlation of results of annealing experiments conducted in the JEM-2000FX TEM with those of chemical-etching studies remains unresolved at this time. It is not clear if the change in annealing rate represents a change in the annealing mechanism or the separate influences of radiolytic and thermal annealing processes.

Acknowledgments

T.P. receives support from the Francis Xanders Memorial Scholarship, the Women's Auxiliary of the American Institute of Mining and Engineering, and ASU Graduate Student Association grant CIRD571. P.F. acknowledges support from National Science Foundation grants DPP8821937 and DPP8816655. Irradiation of Durango apatite was conducted at the Georgia Institute of Technology. P. Green was an invaluable consultant during the course of this study. The authors also thank the supportive staff of the NSF-ASU Facility for HREM, S. Bergman, D. Smith, R. Walker, and G. Wolf, for discussion and review of an early version of the manuscript and A. Hurford, L. Bursill, and R. Angel for their contributions to the final manuscript.

References cited

Bursill, L.A., and Braunshausen, G. (1991) Heavy-iron irradiation tracks in zircon. Philosophical Magazine, 62(4), 395–420.

Carlson, W.D. (1990) Mechanisms and kinetics of apatite fission-track annealing. American Mineralogist, 75, 1120–1139.

Crowley, K.D. (1986) Neutron dosimetry in fission track analysis. Nuclear Tracks and Radiation Measurement, 11(4–5), 237–243.

Dartyge, E., Duraud, J.P., Langevin, Y., and Maurette, M. (1981) New model of nuclear particle tracks in dielectric minerals. Physical Review B, 23(10), 5213–5229.

Donelick, R.A. (1991) Crystallographic orientation dependence of mean etchable fission track length in apatite: An empirical model and experimental observations. American Mineralogist, 76, 83–91.

Donelick, R.A., Roden, M.K., Mooers, J.D., Carpenter, B.S., and Miller, D.S. (1990) Etchable length reduction of induced fission tracks in apatite at room temperature (~23 °C): Crystallographic orientation effects and "initial" mean lengths. Nuclear Tracks and Radiation Measurement, 17(3), 261–267.

Draganic, I.G., Draganic, Z.D., and Adloff, J.-P. (1989) Radiation and radioactivity on Earth and beyond, p. 107–127, 247–261. CRC Press, Boca Raton, Florida.

Duddy, I.R., Green, P.F., and Laslett, G.M. (1988) Thermal annealing of fission tracks in apatite: 3. Variable temperature behaviour. Chemical Geology, Isotope Geoscience Section, 73, 25–38.

Fitzgerald, P.G., and Gleadow, A.J.W. (1990) New approaches in fission track geochronology as a tectonic tool: Examples from the Transantarctic Mountains. Nuclear Tracks and Radiation Measurement, 17(2), 351–357.

Fleischer, R.L., Price, P.B., and Walker, R.M. (1975) Nuclear tracks in solids: Principles and applications, 548 p. University of California Press, Berkeley, California.

Gleadwo, A.J.W., Duddy, I.R., and Lovering, J.F. (1983) Fission track analysis: A new tool for the evaluation of thermal histories and hydrocarbon potential. Petroleum Exploration Association of Australia Journal, 23, 9–102.

Gleadow, A.J.W., Duddy, I.R., Green, P.F., and Hegarty, K.A. (1986a) Fission track lengths in the apatite annealing zone and the interpretation of mixed ages. Earth and Planetary Science Letters, 78, 245–254.

Gleadow, A.J.W., Duddy, I.R., Green, P.F., and Lovering, J.F. (1986b) Confined fission track lengths in apatite: A diagnostic tool for thermal history analysis. Contributions to Mineralogy and Petrology, 94, 405–415.

Green, P.F. (1981) "Track-in-track" length measurements in annealed apatites. Nuclear Tracks and Radiation Measurement, 5(1–2), 121–128.

Green, P.F., and Durrani, S.A. (1977) Annealing studies of tracks in crystals. Nuclear Tracks and Radiation Measurement, 1(1), 33–39.

Green, P.F., and Hurford, A.J. (1984) Thermal neutron dosimetry for fission track dating. Nuclear Tracks and Radiation Damage, 9(3–4), 231–241.

Green, P.F., Duddy, I.R., Gleadow, A.J.W., Tingate, P.R., and Laslett, G.M. (1986) Thermal annealing of fission tracks in apatite: 1. A qualitative description. Chemical Geology, Isotope Geoscience Section, 59, 237–253.

Green, P.F., Duddy, I.R., and Laslett, G.M. (1988) Can fission track annealing in apatite be described by first-order kinetics? Earth and Planetary Science Letters, 87, 216–228.

Green, P.F., Duddy, I.R., Laslett, G.M., Hegarty, K.A., Gleadow, A.J.W., and Lovering, J.F. (1989) Thermal annealing of fission tracks in apatite: 4. Quantitative modelling techniques and extension to geological timescales. Chemical Geology, Isotope Geoscience Section, 79, 155–182.

Hepburn, C., and Windle, A.H. (1980) Review: Solid state nuclear track detectors. Journal of Materials Science, 15, 279–301.

Hirsch, P., Howie, A., Nicholson, R.B., Pashley, D.W., and Whelan, M.J. (1965) Electron microscopy of thin crystals, 561 p. Robert E. Krieger Publishing Company, Malabar, Florida.

Hobbs, L.W. (1987) Electron-beam sensitivity in inorganic specimens. Ultramicroscopy, 23, 339–344.

Hughes, J.M., Cameron, M., and Crowley, K.D. (1990) Crystal structures of natural ternary apatites: Solid solution in the $Ca_5(PO_4)_3X$ (X = F, OH, Cl) system. American Mineralogist, 75, 295–304.

Hull, D., and Bacon, D.J. (1984) Introduction to dislocations. International series on materials science and technology (3rd edition), p. 1–37. Pergamon Press, Oxford, England.

Hurford, A.J. (1990) Standardization of fission track dating calibration: Recommendation by the Fission Track Working Group of the I.U.G.S. Subcommission on Geochronology. Chemical Geology, Isotope Geoscience Section, 80, 171–178.

Laslett, G.M., Green, P.F., Duddy, I.R., and Gleadow, A.J.W. (1987) Thermal annealing of fission tracks in apatite: 2. A quantitative analysis. Chemical Geology, Isotope Geoscience Section, 65, 1–13.

McConnell, D. (1973) Apatite: Its crystal chemistry, mineralogy, utilization, and geologic and biologic occurrences, p. 1–106. Springer-Verlag, New York.

Naeser, C.W. (1979) Thermal history of sedimentary basins: Fission track dating of subsurface rocks. Society of Economic Paleontologists and Mineralogists Special Publication, 26, 109–112.

Pappas, A.C., Alstad, J., and Hagebo, E. (1969) Mass, energy and charge distribution in fission. Physics and chemistry of fission, p. 669–699. International Atomic Energy Agency Press, Vienna, Austria.

Paul, T.A. (1990) A study of fission tracks in apatite using high resolution transmission electron microscopy: A method for the *in-situ* observation of annealing (abs.). Seventh International Congress on Geochronology, Cosmochemistry, and Isotope Geology, Geological Society of Australia, Canberra, Australia, 27, 77.

Paul, T.A., and Fitzgerald, P.G. (1990) Transmission electron microscopy investigation of fission tracks in apatite: A method for the *in-situ* ob-

servation of annealing. Geological Society of America Abstracts with Program, 22(7), 216.

Price, P.B., and Walker, R.M. (1962) Chemical etching of charged particle tracks. Journal of Applied Physics, 33, 3407–3412.

Seiber, K.G. (1986) Structure of the lower Cretaceous sediments—Fish Creek—Victoria, and compositional variation in apatites, 85 p. B.Sc.(hons.) thesis, University of Melbourne, Melbourne, Australia.

Silk, E.C.H., and Barnes, R.S. (1959) Examination of fission fragment tracks with electron microscopy. Philosophical Magazine, 4, 970–972.

Yoon, H.S., and Newnham, R.E. (1969) Elastic properties of fluorapatite. American Mineralogist, 54, 1193–1197.

Young, D.A. (1958) Etching of radiation damage in lithium fluoride. Nature, 182, 375–377.

Young, E., Myers, A.T., Munson, E.L., and Conklin, N.M. (1969) Mineralogy and geochemistry of fluorapatite from Cerro De Mercado, Durango, Mexico. U.S. Geological Society Professional Paper, 650D, D84–D93.

Zoltai, T., and Stout, J.H. (1984) Mineralogy concepts and principles, p. 447–455. Burgess Publishing Company, Minneapolis, Minnesota.

Manuscript received July 8, 1991
Manuscript accepted November 11, 1991